Available online at www.sciencedirect.com

SciVerse ScienceDirect

Ceramics International 38 (2012) 1563–1570

CERAMICS INTERNATIONAL

www.elsevier.com/locate/ceramint

New block graft of α-TCP with silicon in critical size defects in rabbits: Chemical characterization, histological, histomorphometric and micro-CT study

Jose E. Mate-Sanchez de Val [a,*], Jose L. Calvo-Guirado [b], Rafael A. Delgado-Ruiz [a], Ma P. Ramirez-Fernandez [b], Isabel M. Martinez [c], Jose Manuel Granero-Marin [d], Bruno Negri [b], Fernando Chiva-Garcia [a], Jose Maria Martinez-Gonzalez [e], Piedad N. de Aza [c]

[a] Department of Restorative Dentistry, Faculty of Medicine and Dentistry, University of Murcia, Murcia, Spain
[b] Department of Implant Dentistry, Faculty of Medicine and Dentistry, University of Murcia, Murcia, Spain
[c] Bioengineering institute, Miguel Hernandez University, Elche, Spain
[d] Department of General Dentistry, Faculty of Medicine and Dentistry, University of Murcia, Murcia, Spain
[e] Department of Oral Surgery, Faculty of Medicine and Dentistry, University of Madrid, Madrid, Spain

Received 12 July 2011; received in revised form 20 September 2011; accepted 21 September 2011
Available online 28 September 2011

Abstract

The study characterized Si-containing α-TCP blocks designed for graft application and examined their osseintegration in rabbit tibiae using histological, histomorphometric and micro-CT techniques. The block grafts were inserted into the critical size defects of 15 rabbits, using both tibiae, and examined at 15, 30 and 60 days. Results showed that new bone grew in direct contact with the block grafts and that the presence of silicon improved the stability and osseointegration of the material. Silicon doped TCP grafts showed enhanced mesenchymal cell differentiation and increased osteoblast activity compared with α-TCP. Furthermore, blocks with the highest concentration of silicon (3% C_2S, 97% TCP) showed better dimensional stability and increased bone-to-implant contact values after 60 days (67.6 ± 5% lateral bone contact and 57.3 ± 3% base bone contact). None of the implanted materials were seen to produce any adverse inflammation. The study found that α-TCP ceramic blocks containing 3% C_2S, offer good bioactivity, biocompatibility and allow new bone growth around the block and within the graft body, making this an ideal block graft material.

Key words : Block graft; Bone substitute; Calcium phosphates; Silicon; Tricalcium phosphate

1. Introduction

Bioceramics, especially calcium phosphate ceramics, have been widely used for bone tissue repair in orthopedic and dental applications due to their good biocompatibility and osteoconductivity [1–5]. Commercial calcium phosphate bioceramics are usually composed of hydroxyapatite ($Ca_{10-x}(HPO_4)_x(PO_4)_{6-x}(OH)_{2-x}$, with $0 \leq x \leq 1$), β-tricalcium phosphate (β-$Ca_3(PO_4)_2$) or their admixture, known as HA, β-TCP, and biphasic calcium phosphate (BCP), respectively [6,7]. In spite of these positive qualities, the bioresorption rate of HA bioceramics is very slow and they remain undegraded several years after implantation [8]. Although BCP and β-TCP are more resorbable than HA bioceramics, an even higher resorption rate is desirable for bone repairing applications whenever complete implant osseointegration and replacement is required in the mid-term. Over the last decade, intensive research has been devoted to the preparation of ion-substituted calcium phosphate materials with the aim of improving osteogenesis, resorption rates and strength [9–11]. Particularly, Si [12,13] and Mg [14,15] have received a great deal of attention as substitutes for calcium phosphates in biomedical applications, specifically in HA and TCP. Recent research has

* Corresponding author at: C\ Marques de los Velez s/n, Zip Code: 03004, Murcia, Spain. Tel.: +34 637 477 932.
E-mail address: josemate@um.es (J.E. Mate-Sanchez de Val).

0272-8842/$36.00
doi:10.1016/j.ceramint.2011.09.042

shown that dietary silicon intake is positively associated with cortical mineral density, which is subject to the availability of estrogens [16]. Furthermore, silicon-doped TCP cement has shown enhanced mesenchymal cell differentiation and increased osteoblast activity compared with α-TCP [17].

The use of xenografts in blocks for the replacement of large volumes of bone is an important research field because of the complications and morbidity of autologous graft techniques. Such techniques allow the vertical raising of atrophic areas without resorting to autologous bone grafts [18]. The possibility of adding osteoinductive bioactive components that allow greater integration of the block, preventing its loss and encapsulation, has become another focus of recent study. The addition of silicon to TCP can improve stability, provide better structural properties and stimulate new bone formation [19]. Taking these factors into consideration, calcium phosphates with Si substitutions offer themselves as promising candidates for the preparation of bioceramics with improved osteogenic properties. TCP is more soluble and biodegradable than HA, as Si ions occupying P sites in the TCP network are more labile than in the HA network. Dissolution and biodegradation rates are in the order of α-TCP > β-TCP > HA and they can be strongly influenced by ion substitutions. Si is also a recognized stabilizer of the α-phase [20,21], so controlled Si-doping has been proposed as a way to improve the mechanical strength of TCP bioceramics [22].

The hypothesis under examination in the present study is that TCP with silicon in solid solution (TCPss) ought to be more reactive than α-TCP because of its greater solubility in physiological fluids and its lower lattice packing. The aim of this research, therefore, was to investigate whether new blocks of TCPss with different concentrations of Si stimulate bone deposition on their surfaces, coupled with osteoclastic cell resorption and/or biodegradation when implanted into critical size defects (6 mm Ø) in rabbit tibiae, comparing this material with synthetic pure α-TCP and analyzing all study samples by means of histological, histomorphometric and micro-CT techniques.

2. Materials and methods

2.1. Materials and composition

The starting materials for the present study were previously synthesized TCP and C_2S. Tricalcium phosphate was synthesized by solid state reaction of a stoichiometric mixture of calcium hydrogen phosphate anhydrous ($CaHPO_4$, Panreac) and calcium carbonate ($CaCO_3$, Fluka) with an average particle size of <15 £gm. The mixture of $CaHPO_4$ and $CaCO_3$ was heated in a platinum crucible at 1500 °C for 3 h. It was then liquid nitrogen-quenched after rapid removal from the furnace. The final product was ground and characterized by X-ray diffraction (XRD).

Dicalcium silicate was obtained by solid-state reaction-sintering, starting from an appropriate mixture of calcium carbonate ($CaCO_3$ > 99.0 wt% Fluka) with an average particle size of <15 μm, and silicon oxide (SiO_2 > 99.7 wt%, Strem Chemicals) with an average particle size <50 μm. As a preliminary step, SiO_2 was wet ground in a laboratory mixing miller (MM301-Retsch) by using PSZ-zirconia balls and isopropyl alcohol as a suspension medium. The powder was then dried and sieved to <50 μm. The average particle size of the SiO_2 was 40 μm as measured by laser diffraction (Mastersizer2000E device – Malvern). Next, the desired proportions of the constituents were weighed out and thoroughly wet mixed in a mixing miller with the same PSZ balls mentioned above as the grinding medium. After the milling process, the mixture was dried and burned at 1000 °C for 24 h to remove CO_2. Then, this powder was isostatically cold pressed at 200 MPa and heat-treated at 1525 °C for 12 h, at a heating rate of 8.3 °C/min followed by a cooling rate of 5 °C/min. The reaction-sintering temperature was selected according to information provided by the SiO_2–CaO phase equilibrium diagram evaluated and reported by Eriksson et al. [23]. The material was ground and characterized by XRD. Mixtures with compositions of 0 wt%, 1.5 wt% and 3.0 wt% of C_2S were prepared. First, TCP and C_2S powders were ground to an average particle size of 25 μm and 20 μm respectively, and the desired proportions of each component were weighed in an analytical balance and thoroughly mixed in a manual agate mortar under acetone. They were then isostatically pressed into bars at 200 MPa. The Si-containing TCP (TCPss) bars were heated up to 1500 °C/2 h and then liquid-nitrogen quenched after rapid removal from the furnace. The bars were then ground, pressed and reheated again. This procedure was repeated three times in order to homogenize the compositions. After homogenization, the samples were pressed at 200 MPa and heated up to 1500 °C where they were held for 4 h. Samples were then cooled down inside the furnace to 1120 °C, at a rate of 3.2 °C/min, and held at this temperature for a period of 16 h followed by slow cooling to room temperature at a rate of 6.2 °C/min.

2.2. Material characterization

XRD analysis was carried out (Bruker-AXS D8Advance) to determine the crystalline phases of the different compositions. XRD patterns were recorded from θ to 2θ scans in para-focusing Bragg–Brentano geometry with line focused copper Kα ($\lambda_{CuK\alpha1}$ = 1.54056 Å) radiation from a conventional sealed tube source. The diffractometer was equipped with a scintillation detector. Scans were taken from 10° to 40° (2θ) in 0.05° steps with counting times of 6 s per step. As X-ray diffraction is sensitive to crystallite size, the Scherrer formula was used to determine the crystallite size of each material.

The microstructures of the sintered samples were studied using specimens polished down to 1 μm with diamond paste and chemically etched with diluted acetic acid (1.0%, v/v) for 6 s. Samples were then gently cleaned in an ultrasonic bath with distilled water, dried and palladium coated for scanning electron microscopy observations (SEM-Hitachi S-3500N). Quantitative analyses were made by a Wavelength Dispersive X-ray Spectroscopy (WDS) system coupled to the electron microscope, using ZAF (atomic number, absorption, fluorescence) correction

software and TCP Bayer standards. The final microanalysis data represented the mean average of ten independent determinations.

2.3. Material properties

Three groups of cylindrical implants (6 ± 0.01 mm in diameter and 8 ± 0.01 mm in length) were studied, with varying Si composition: A: 97 TCP – 3% C_2S; B: 98.5 TCP – 1.5% C_2S; C: 100 TCP – 0% C_2S. These were distributed randomly amongst critical size defects by means of random number generator software, SPSSR v.18.0. (IBM Corporation, New York, United States).

2.4. Animal experimentation

2.4.1. Main protocol

The study protocol was approved by the Animal Ethics Committee of the University of Murcia, following Spanish Government and European Community Guidelines for animal care. 15 male New Zealand rabbits of 3.5–4.5 kg in weight were used, divided into three groups ($n_1 = 5$, $n_2 = 5$, $n_3 = 5$) corresponding to study times of 15, 30 and 60 days. Both tibiae were used for the implantation of the three material variations. The animals received an intramuscular injection of 0.5 to 1 mg/kg acepromazine maleate. General anesthesia included ketamine plus chlorbutol (5–8 mg/kg intravenously), 0.5–1 mg/kg acepromazine maleate as a coadjuvant and 0.05 mg/kg atropine. Amoxycillin (0.1 ml/kg intramuscularly) was administered at the end of the surgery.

2.4.2. Surgical procedure

Two critical defects (6 mm Ø) were created in the proximal zone of both tibiae, making a total of 60. The surgical approach was in the proximal metaphyseal–diaphyseal area of the tibia, several millimeters below the anterior tibial tuberosity. Bone tissue was removed with spherical surgical drills of 6 mm in diameter at low rotation speed with constant irrigation.

2.5. Histology and histomorphometric analysis

After the elapse of the implantation time, the implants with the surrounding tissues were removed and fixed in 10% neutral buffered formalin and decalcified. The decalcification method utilized OsteomolR Merck KbaA (Germany) containing HCl (10%) and CH_2O (4%), immersing samples for 17 days and renewing the solution every 24 h. Subsequently, all samples were paraffin embedded, sectioned at 5 μm and stained using Hematoxylin–Eosin. The entire circumference of each section (containing bone, grafted particles, and connective tissue) was traced manually to create an individual region-of-interest (ROI). Histomorphometric evaluations consisted of measurements of the area of graft material in relation to the total measurement area.

Histomorphometric measurement of the samples was carried out using Image J software (developed by the National Institute of Health [NIH] of the United States of America). Examinations were performed under a Nikon Elipse 80i microscope (Teknooptik AB, Huddinge, Sweden) equipped with an Easy Image 2000 system (Teknooptik AB) using 10× to 40× lenses for descriptive evaluation and morphometric measurement. Images were generated using a Leica Z6 APO microscope connected to a Leica DC 500 (Barcelona, Spain) digital camera, enlarged 23×. After calibrating the system and digitalizing images, interactive measurements of the areas of interest were obtained using image analysis software Leica QWin V3 (Barcelona, Spain). Histomorphometric analysis produced two measurements: LBC (lateral bone contact: percentage of bone in contact with lateral side of graft) and BBC (base bone contact: percentage of bone in contact with the graft base) (Fig. 1).

2.6. Micro-CT

Micro-CT analysis was performed using the CT SkyScan 1172 system, allowing accurate imaging, with resolution of less than 5 μm and 3D measurement capability. Analysis variables are represented in Table 1. The samples were cut into blocks using a diamond blade of 0.1 mm thickness and 22 mm diameter (Komet Group, Lembo, Germany), leaving a 3 mm safety margin on both sides of the grafts in order to keep the grafts intact. All implant sites were analyzed as follows:

Bone Volume Fraction (BV/TV), known as bone volume fraction or percentage of bone volume, expresses the percentage of the volume analyzed occupied by bony structures (TV: total volume).

Intersection Surface (IS) introduces the additional dimension of depth to the analysis of bone-to-implant contact. The contact area is measured as a profile to show greater or lesser distance from the implant surface. IS profiles are usually expressed as percentages of bone contact surface in relation to the total areas (IS/TS).

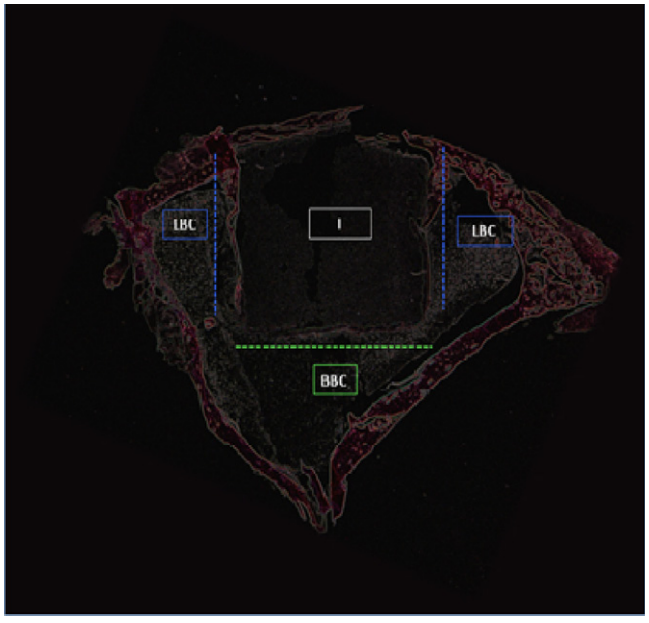

Fig. 1. Histological characterization for histomorphometric analysis.

Table 1
Technical characteristics of Micro-CT.

Voltage	100 kV
Intensity	100 μA
Pixel size	10.90 μm
Frame averaging	2
Random movement	10

The μ-CT images represent a 3D reconstruction generated from CT images of the bone graft, with resorption and the space between block graft and host bone measured in microns. The color scale represents the space between the block and the host bone.

2.7. Statistical analysis

Statistical analysis was performed using PASW Statistics v.18.0.0 software (SPSS Inc.). Values were recorded as mean ± standard deviation, to examine the effects of the material on the histomorphometry parameters BV and IS, as well as lateral bone and graft base contact (LBC and BBC). Student's *t*-test was applied to the comparison of mean averages and to quantify relationships between differences. Student's *t*-test was also applied to histomorphometric analysis and micro-CT values to analyze differences between the mean values. Equal means were regarded as the null hypothesis, whilst the existence of significant differences between means acted as an alternative hypothesis. As significant differences between the means existed, the null hypothesis was rejected.

3. Results

3.1. Ceramic characterization

Fig. 2 shows XRD patterns of the materials 100-TCP, 98.5-TCP and 97-TCP. It can be seen that the polymorphic form of α-TCP corresponds to JCPDS card no. 9-348. Regardless of the addition of C_2S, XRD patterns of TCP doped with different amounts of C_2S show only peaks corresponding with α-TCP (JCPDS card no. 9-348). XRD patterns show that grain size decreased as Si content increased from 207 nm for the pure α-TCP to 194 nm and 129 nm for 98.5-TCP and 97-TCP respectively. Fig. 3 shows polished and etched surfaces of pure 100-TCP (a), 98.5-TCP (b) and 97-TCP (c). No significant microstructural features are visible except for closed pores with an average size of 20 μm. The total porosity of the samples was not seen to change as a result of varying C_2S content. Microphotographs show that samples only present one phase, with C_2S in solid solution, as detected by WDS. This finding is in perfect agreement with the XRD results in which a single α-TCP phase was detected. WDS analysis (Table 2) shows the composition of the TCPss studied in terms of wt% of Si.

3.2. Histological analysis

Analyses of histological sections were performed at 15, 30 and 60 days for each of the three materials studied, examining resorption type and new bone formation. None of the grafted materials elicited a significant inflammatory reaction. In all samples, woven bone was identified around and in close contact with the material and, as might be expected in rabbit tibial bone, small marrow spaces were observed in the peri-material bone, reaching maturity after 60 days. 97-TCP implants showed slower resorption than the other groups, 98.5-TCP and 100-TCP. After 15 days the block of 97-TCP was partially resorbed both peripherally and within the graft body, with slight new bone formation around it (Fig. 4a). Material degradation was more evident at 30 and 60 days, the volume of the block of 97-TCP implant decreasing progressively (Fig. 4b) as bone formation increased at the periphery and within the block, leading to its virtual disappearance and almost complete closure of the cortex at 60 days (Fig. 4c).

In blocks of 98.5-TCP, histological results showed that after 15 days of implantation the changes related to residual block

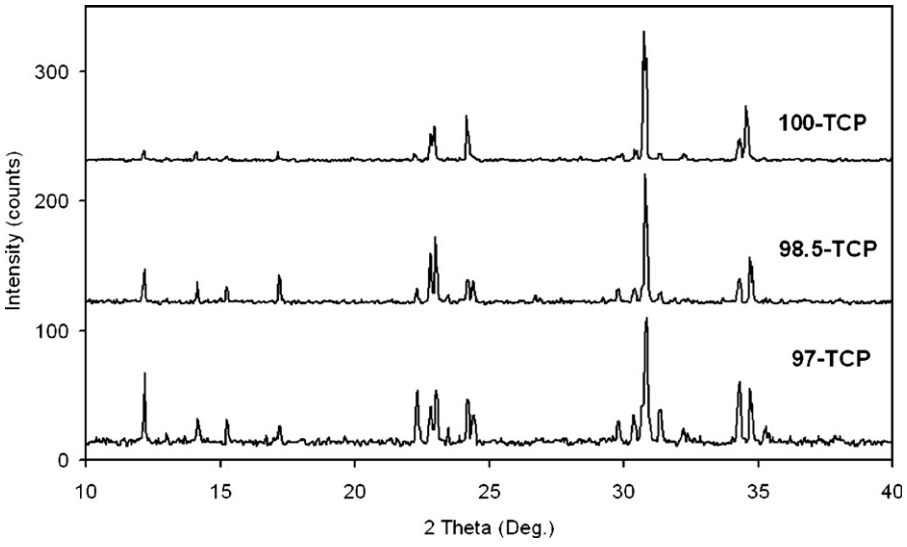

Fig. 2. XRD patterns of the materials 100-TCP, 98.5-TCP and 97-TCP.

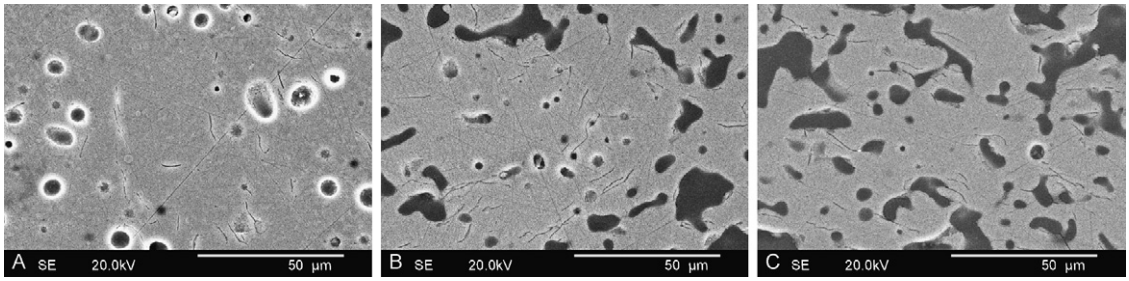

Fig. 3. Polished and etched surfaces of pure 100-TCP (a), 98.5-TCP (b) and 97-TCP (c).

Table 2
Composition of the TCPss studied in terms of wt% of Si.

Symbol	Weight % Si
α-TCP	0.00
98.5-TCPss	0.24
97.0-TCPss	0.29

content, peripheral bone resorption, new bone formation and closure of the cortex were minimal, in comparison with the other graft compositions (Fig. 4d). This pattern was more evident when comparisons were made between 98.5-TCP grafts at 30 (Fig. 4e) and 60 days (Fig. 4f).

In tibiae treated with 100-TCP blocks, there was less block stability, much greater resorption of the implant and a lower rate of neoformation. At 15 days (Fig. 4g) a higher resorption rate was observed than for blocks of 97-TCP and 98.5-TCP and defect closure was poor. At 30 days (Fig. 4h) a higher resorption rate was also observed than for blocks of 97-TCP and 98.5-TCP. After 60 days (Fig. 4i) the blocks showed extensive peripheral bone resorption (Table 3).

3.3. Micro-CT

Micro-CT analysis pointed to the same conclusions as histological study, observing less dimensional stability, higher resorption and less bone-to-implant contact over the study period as the percentage of α-TCP silicon content decreased. The outlining of pixels measured the presence or absence of bone at different distances from the material, determining the distance at which bone was present. The incorporation of silicon into the graft material achieved a more appropriate and progressive bone turnover both in terms of quantity and time. Micro-CT images of the 97-TCP group showed very little peripheral resorption of the block graft and a minimum area of separation and therefore higher bone-to-implant contact. This scenario was maintained at 30 and 60 days (Fig. 5a–c). 98.5-TCP blocks showed slight resorption at the periphery and within the graft, but this was much less than in 100-TCP samples (Fig. 5d–f). Lastly, for 100-TCP blocks, resorption was very evident and faster over the study time; the gaps between bone and graft were significantly larger indicating lower bone-to-graft contact (Fig. 5g–i).

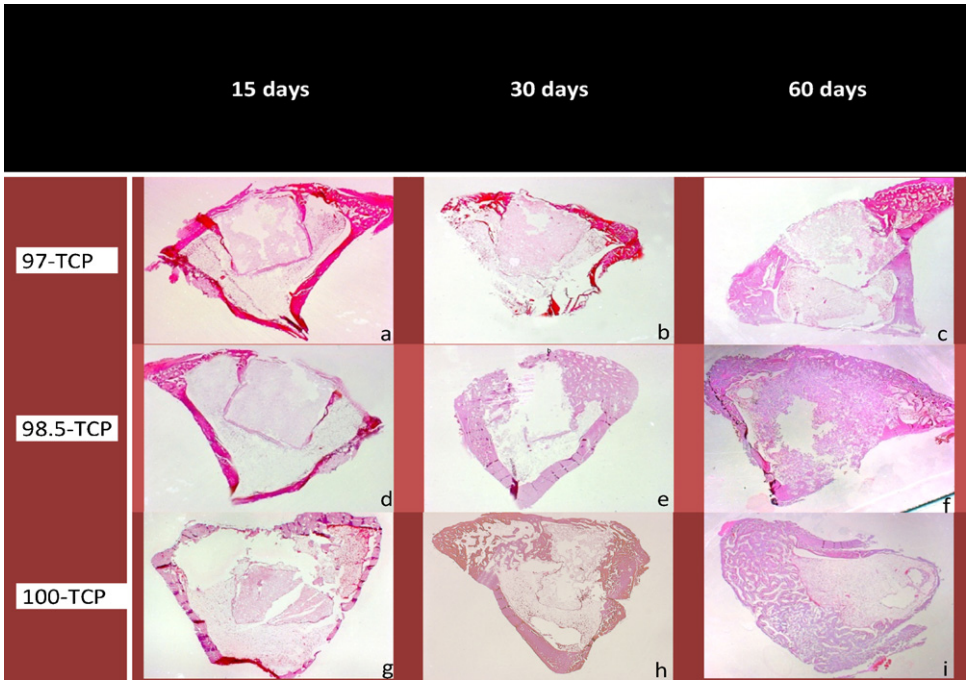

Fig. 4. Histological material comparison with different concentrations of silicon (23× magnification).

Table 3
% of reabsorption rate.

Days	97	98.5	100
15	93.5	92	65.2
30	69.8	67.2	58.5
60	57.8*	34.71	28.5

* Significant differences ($P < 0.05$).

Micro-CT analysis of BV/TV (bone volume fraction) and IS (bone-to-implant contact) provided additional information (Table 4) as follows.

Significant differences in BV/TV values in favor of 97-TCP were found across all study periods, with higher bone volume percentages compared to the control, with the biggest difference recorded for 97-TCP at 60 days. Significant differences were also found between IS values (bone-implant contact) in favor of 97-TCP, which was more evident at 60 days.

3.4. Histomorphometry

Histomorphometric analysis revealed higher bone-to-implant contact values for 97-TCP, so that LBC increased significantly across the study times at 15, 30 and 60 days (30.4 ± 3 vs 43 ± 2 vs 67.6 ± 5). Significantly higher BBC contact values were also found for 97-TCP at 60 days in comparison with the other study groups (57.3 ± 5 vs 35.4 ± 2 and 45.8 ± 2). These findings point to greater interaction between the host bone and graft and agree with data obtained in the histology and micro-CT analyses (Table 5). The differences between the groups and within each group were analyzed statistically, showing significant differences between LBC and BBC values obtained for 97-TCP grafts at 60 days, 30 days, and 15 days. There were also significant differences between 97-TCP and 98.5-TCP data at 15, 30 and 60 days and in comparison with samples treated with 100-TCP.

Table 4
Micro-CT analysis of BV/TV (bone volume fraction) and IS (bone-to-implant contact).

Days	Pixel	97-TCP		98.5-TCP		100-TCP	
		BV/TV	IS/TS	BV/TV	IS/TS	BV/TV	IS/TS
15	0–10	68.32*	48.29*	60.39	43.17	31.56	41.32
	10–20	88.23*	69.21*	77.31	64.65	14.49	50.56
30	0–10	69.89*	49.32	63.32	45.62	35.23	46.32
	10–20	89.32*	68.32*	79.32	66.98	19.32	58.99
60	0–10	72.32*	71.32*	65.32	47.63	42.21	49.65
	10–20	91.23*	82.23*	71.32	69.32	21.23	60.16

* Significant differences ($P < 0.05$).

4. Discussion

α-TCP remains metastable at room temperature and XRD data proved that only α polymorph was present in the sintered TCP and TCPss samples. Furthermore, SEM micrographs and WDS analysis showed that only one homogeneous phase was present in the compositions studied. These findings agree with other data reported in the literature [24]. It is important to note that this low level of C_2S substitution had a strong effect on α-TCP's thermal stability. Previous studies have reported that the transition of pure β-TCP to α-TCP occurs at 1125 °C, so the addition of C_2S lowered this phase transition temperature.

Vertical bone volume augmentation is a focus of much biomaterial research and development, aimed at bone volume restoration in atrophic ridges [25]. α-TCP with silicon in block form offers biocompatibility and does not produce any adverse inflammatory reactions at the insertion site, the fact that it is

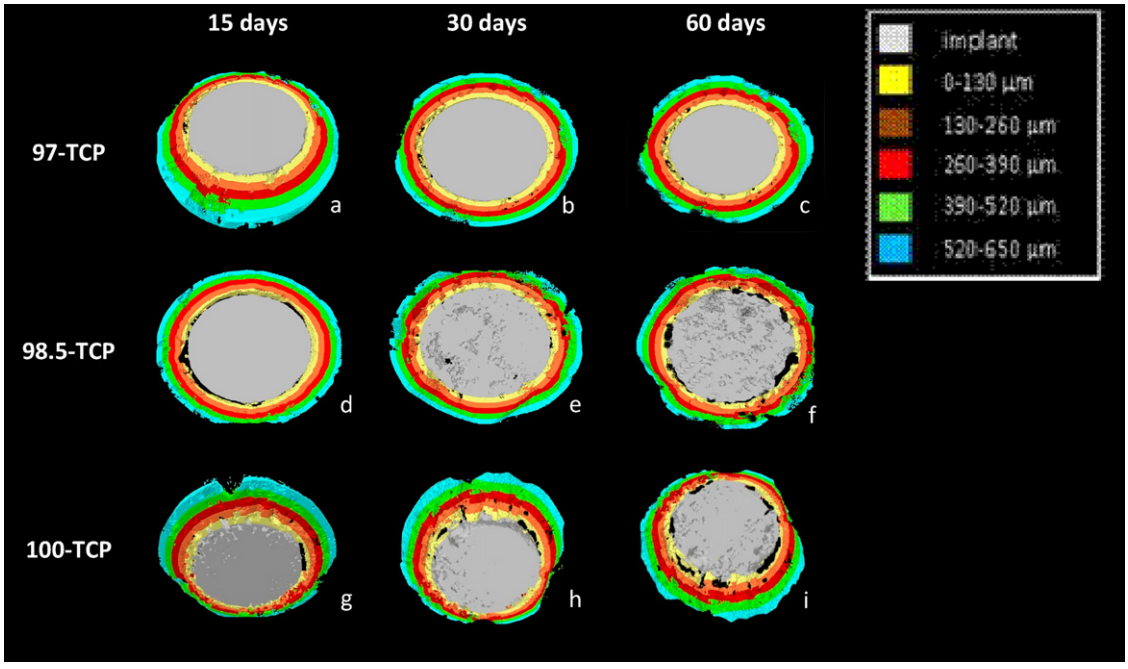

Fig. 5. Micro-CT material comparison with different concentrations of silicon.

Table 5
Histomorphometric analysis of bone-graft contact.

Graft material	LBC ± SD			BBC ± SD		
	15 d	30 d	60 d	15 d	30 d	60 d
97-TCP	30.4 ± 3%	43 ± 2%*	67.6 ± 5%*	35.4 ± 2%	45.8 ± 2%*	57.3 ± 5%*
98.5-TCP	23.6 ± 5%	28.3 ± 4%	43.7 ± 8%*	26.8 ± 2%	38.2 ± 4%	44.6 ± 1%*
100-TCP	15.8 ± 3%	26.5 ± 2%	40.5 ± 4%	21.4 ± 3%	33.6 ± 4%	38.7 ± 2%

* Significant differences ($P < 0.05$).

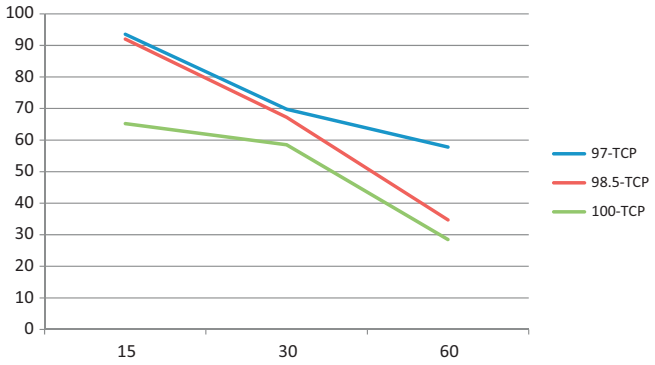

Fig. 6. Material reabsorption rates. (%).

absorbable allows its rapid replacement by new bone, without causing any reactions to foreign bodies. For this reason, little or no inflammatory reaction was observed, which was similar to the control samples. The material has sufficient mechanical strength and resorbs at a good rate (Fig. 6, Table 6) guaranteeing replacement by autologous bone [26]. Its rapid replacement by new bone allows a bone matrix to become established within the material giving the receiving area physical properties similar to the bone. α-TCPss stabilized in cylinder form allows the precise evaluation of resorption, dimensional stability and its replacement by new bone [27]. The incorporation of silicon improves the material's integration and compatibility, accelerates bone replacement and enhances the properties of pure α-TCP, which is otherwise resorbed too quickly and is less stable [27]. It is known that an appropriate concentration of silicon in this biomaterial acts as an integration stimulant, promoting bone matrix and ion exchange with the implant environment [28]. Histological analysis of the blocks at 15, 30 and 60 days showed normal bone growth patterns and an absence of abnormal inflammatory cells. The formation of osteocytes lacunae and new bone maturation indicated normal healing processes and rapid biological response in the new bone [29,30]. According to Trojani et al. [31], in an in vivo experimental model, the material produced appropriate bone replacement, cell differentiation and stimulated osteoblasts, the authors observing greater amounts of mineralized bone and increased osteoblast activity. As revealed by micro-CT examination, higher concentrations of silicon in α-TCP achieved greater interaction with peripheral new bone, higher percentages of bone-to-graft contact and higher percentages of the total volume of bone. Histomorphometry showed higher rates of bone-to-graft contact on both the base and sides of the graft when silicon content was increased [32]. Despite the New Zealand rabbit's rapid metabolic activity, other studies have established its validity as an experimental model for testing biomaterials used for bone replacement [33]. In this way, values obtained are enhanced through the creation of critical defects of 6 mm diameter, which will not close spontaneously and therefore demonstrate the regenerative potential of α-TCP biomaterial [34].

Table 6
Mechanical properties of the samples.

	HK	HV	E (GPa)
100 TCP	0.27 ± 0.5	0.61 ± 0.5	24.3 ± 0.5
98.5 TCP	0.28 ± 0.5	0.62 ± 0.5	24.4 ± 0.5
97 TCP	0.32 ± 0.5	0.63 ± 0.5	24.6 ± 0.5

HV: Vickers hardness, HK: Knoop hardness, E: Elasticity.

5. Conclusions

TCP block grafts with 3% C_2S are a valid and effective alternative to other materials used for bone volume replacement and the regeneration of bone atrophy. The material offers an ideal matrix in regenerative procedures because of its initial dimensional stability (93.5% material remaining at 15 days), resorption rate (57.8% material remaining at 60 days), its stimulation of bone formation and bone to implant contact (67.6 ± 5% LBC and 57.3 ± 5% BBC at 60 days), and eventual replacement by autologous bone.

Acknowledgements

Part of this work was supported by CICYT, project no. MAT2006-12749-C02-02.

References

[1] R. Xin, Y. Leng, J. Chen, Q. Zhang, A comparative study of calcium phosphate formation on bioceramics in vitro and in vivo, Biomaterials 26 (2005) 6477–6486.
[2] A. Ramila, M. Vallet-Regi, Static and dynamic in vitro study of a sol–gel glass bioactivity, Biomaterials 22 (2001) 2301–2306.
[3] C.V. Ragel, M. Vallet-Regi, L.M. Rodriguez-Lorenzo, Preparation and in vitro bioactivity of hydroxyapatite/solgel glass biphasic material, Biomaterials 23 (2002) 1865–1872.
[4] S. Fujibayashi, M. Neo, H.M. Kim, T. Kokubo, T. Nakamura, A comparative study between in vivo bone in growth and in vitro apatite formation on Na_2O–CaO–SiO_2 glasses, Biomaterials 24 (2003) 1349–1356.
[5] P. Siriphannon, Y. Kameshima, A. Yasumori, K. Okada, S. Hayashi, Comparative study of the formation of hydroxyapatite in simulated body

fluid under static and flowing systems, Journal of Biomedical Materials Research 60 (2002) 175–185.
[6] P.N. De Aza, A.H. De Aza, S. De Aza, Crystalline bioceramic materials, Boletin de la Sociedad Española de Cerámica y Vidrio 44 (2005) 135–145.
[7] R.Z. LeGeros, S. Lin, R. Rohanizadeh, D. Mijares, J.P. LeGeros, Biphasic calcium phosphate bioceramics: preparation, properties and applications, Journal of Materials Science: Materials in Medicine 14 (2003) 201–209.
[8] S.V. Dorozhkin, In vitro mineralization of silicon containing calcium phosphate bioceramics, Journal of the American Ceramic Society 90 (2007) 244–249.
[9] S.M. Best, S. Zou, R. Brooks, J. Huang, N. Rushton, W. Bonfield, The osteogenic behaviour of silicon substituted hydroxyapatite, Key Engineering Materials 36 (2008) 1–363, 985–988.
[10] E.S. Thian, J. Huang, S.M. Best, Z.H. Barber, W. Bonfield, Silicon-substituted hydroxyapatite: the next generation of bioactive coatings, Materials Science and Engineering C 27 (2007) 251–256, 2007.
[11] C.M. Botelho, R.A. Brooks, S.M. Best, M.A. Lopes, J.D. Santos, N. Rushton, W. Bonfield, Human osteoblast response to silicon-substituted hydroxyapatite, Journal of Biomedical Materials Research Part A 79 (2006) 723–730.
[12] E.S. Thian, J. Huang, M.E. Vickers, S.M. Best, Z.H. Barber, W. Bonfield, Silicon-substituted hydroxyapatite (SiHA): a novel calcium phosphate coating for biomedical applications, Journal of Materials Science 41 (2006) 709–717.
[13] A.E. Porter, N. Patel, J.N. Skepper, S.M. Best, W. Bonfield, Effect of sintered silicate-substituted hydroxyapatite on remodelling processes at the bone–implant interface, Biomaterials 25 (2005), 3303-3014.
[14] E. Landi, G. Logroscino, L. Proietti, A. Tampieri, M. Sandri, S. Sprio, Biomimetic Mg-substituted hydroxyapatite: from synthesis to in vivo behavior, Journal of Materials Science: Materials in Medicine 19 (2008) 239–247.
[15] M. Otsuka, A. Oshinbe, R.Z. Legeros, Y. Tokudome, A. Ito, K. Otsuka, W.I. Higuchi, Efficacy of the injectable calcium phosphate ceramics suspensions containing magnesium, zinc and fluoride on the bone mineral deficiency in ovariectornized rats, Journal of Pharmaceutical Sciences 97 (2008) 421–432.
[16] R. Jugdaohsingh, K.L. Tucker, N. Qiao, L.A. Cupples, D.P. Kiel, J.J. Powell, Dietary silicon intake is positively associated with bone mineral density in men and premenopausal women of the Framingham Offspring cohort, Journal of Bone and Mineral Research 19 (2004) 297–307.
[17] C.L. Camire, S.J. Saint-Jean, C. Mochales, P. Nevsten, J.S. Wang, L. Lidgren, I. McCarthy, M.P. Ginebra, Material characterization and in vivo behavior of silicon substituted α-tricalcium phosphate cement, Journal of Biomedical Materials Research. Part B: Applied Biomaterials 76 (2006) 424–431.
[18] A. Scarano, F. Carinci, B. Assenza, M. Piattelli, G. Murmura, A. Piattelli, Vertical ridge augmentation of atrophic posterior mandible using an inlay technique with a xenograft without miniscrews and miniplates: case series, Clinical Oral Implants Research (2011) 20.
[19] D. Cardaropoli, Vertical ridge augmentation with the use of recombinant human platelet-derived growth factor-BB and bovine bone mineral: a case report, International Journal of Periodontics and Restorative Dentistry 29 (3) (2009) 289–295.
[20] I.M. Martinez, P.A. Velasquez, P.N. De Aza, Synthesis and stability of α-tricalcium phosphate doped with dicalcium silicate in the system $Ca_3(PO_4)_2$–Ca_2SiO_4, Materials Characterization 61 (2010) 761–767.
[21] A.M. Pietak, J.W. Reid, M.J. Stott, M. Sayer, Silicon substitution in the calcium phosphate bioceramics, Biomaterials 28 (2007) 4023–4032.
[22] R. Garcıa-Carrodeguas, A.H. De Aza, X. Turrillas, P. Pena, S. De Aza, New approach to the b-a polymorphic transformation in magnesium-substituted tricalcium phosphate and its practical implications, Journal of the American Ceramic Society 91 (2008) 1281–1286.
[23] G. Eriksson, P. Gu, M. Blander, A.D. Pelton, Critical evaluation and optimisation of the thermodynamic properties and phase diagrams of the MnO–SiO_2 and CaO–SiO_2 systems, Canadian Metallurgical Quarterly 33 (1994) 13–21.
[24] M. Kamitakahara, T. Kurauchi, M. Tanihara, K. Ioku, C. Ohtsuki, Synthesis of Si-containing tricalcium phosphate and its sintering behavior, Key Engineering Materials 361–363 (2008) 59–62.
[25] F. Schwarz, D. Ferrari, E. Balic, D. Buser, J. Becker, M. Sager, Lateral ridge augmentation using equine and bovine derived cancellous bone blocks: a feasibility study in dogs, Clinical Oral Implants Research 21 (9) (2010) 904–912.
[26] D. Ono, R. Jimbo, G. Kawachi, K. Ioku, T. Ikeda, T. Sawase, Lateral bone augmentation with newly developed β-tricalcium phosphate block: an experimental study in the rabbit mandible, Clinical Oral Implants Research (2011) 8.
[27] M. Bohner, Silicon-substituted calcium phosphates – a critical view, Biomaterials 30 (2009) 6403–6406.
[28] A. Balamurugana, A.H. Rebeloa, A.F. Lemosa, J.H. Rochab, J.M. Ventura, J.M. Ferreira, Suitability evaluation of sol–gel derived Si-substituted hydroxyapatite for dental and maxillofacial applications through in vitro osteoblasts response, Dental Materials 24 (2008) 1374–1380.
[29] K. Yamauchi, T. Takahashi, K. Funaki, Y. Hamada, Y. Yamashita, Histological and histomorphometrical comparative study of β-tricalcium phosphate block grafts and periosteal expansion osteogenesis for alveolar bone augmentation, International Journal of Oral Maxillofacial Surgery 39 (10) (2010) 1000–1006.
[30] Y. Anavi, G. Avishai, S. Calderon, D. Allon, Bone remodeling in onlay TCP and coral grafts to rat Calvaria: micro-CT analysis, Journal of Oral Implantology (2010) 16.
[31] C. Trojani, F. Boukhechba, J.C. Scimeca, F. Vandenbos, J.F. Michiels, G. Daculsi, P. Boileau, P. Weiss, G.F. Carle, N. Rochet, Ectopic bone formation using an injectable biphasic calcium phosphate/Si-HPMC hydrogel composite loaded with undifferentiated bone marrow stromal cells, Biomaterials 27 (2006) 3256–3264.
[32] V.S. Komlev, M. Mastrogiacomo, R.C. Pereira, F. Peyrin, F. Rustichelli, R. Cancedda, Biodegradation of porous calcium phosphate scaffolds in an ectopic bone formation model studied by X-ray computed microtomograph, European Cells & Materials Journal 19 (2010) 136–146.
[33] J.L. Calvo-Guirado, R.A. Delgado-Ruíz, M.P. Ramírez-Fernández, J.E. Maté-Sánchez, A. Ortiz-Ruiz, A. Marcus, Histomorphometric and mineral degradation study of Ossceram®: a novel biphasic B-tricalcium phosphate, in critical size defects in rabbits, Clinical Oral Implants Research (2011) 15.
[34] J.L. Calvo-Guirado, M.P. Ramírez-Fernández, G. Gómez-Moreno, J.E. Maté-Sánchez, R. Delgado-Ruiz, J. Guardia, L. López-Marí, A. Barone, A.J. Ortiz-Ruiz, J.M. Martínez-González, L.A. Bravo, Melatonin stimulates the growth of new bone around implants in the tibia of rabbits, Journal of Pineal Research 49 (2010) 356–363.